RSC Advances




ROYAL SOCIETY OF CHEMISTRY

www.rsc.org/advances

# A New Reduction Mechanism of CO Dimer by Hydrogenation into $C_2H_4$ on Cu(100) Surface: A Theoretical Insight into Kinetics of Elementary Steps

Lihui Ou*, Wenqi Long, Yuandao Chen, Junling Jin

**Abstract** A systematic DFT study that examines the role of kinetics of elementary reaction steps during the course of reduction of CO dimer, OCCO* into production $C_2H_4$ on Cu(100) is presented for the first time in the present work, and a new mechanism is introduced. The kinetic analysis of elementary reaction steps have suggested that further reduction of CO is key selectivity-determining step for the formation of $C_2H_4$ and $CH_4$ on Cu(100) and Cu(111). The main reaction pathway on Cu(111) proceeds through reduction of CO into CHO* intermediate, which may eventually result in $CH_x$ species by the breaking of C-O bond, and produce production $CH_4$. On Cu(100), OCCO* is firstly formed by CO dimerization, which is the first step and more favorable pathway than the further hydrogenation of CO. It explains why only $C_2$ species and not $C_1$ species are observed experimentally on Cu(100). For the formation of production $C_2H_4$ on Cu(100), the results suggest that hydrogenation of OCCO* to OCCHO* intermediate is the most possible reaction path, followed by the formation of intermediate OHCCHO* through OCCHO* intermediate further hydrogenation. The formation of OCCO* may be rate-determining step in reduction mechanism of CO dimer. Our present reaction kinetics analysis of elementary steps give a different mechanistic explanation for selectivity of production $C_2H_4$ in contrast to previous suggested thermodynamic theoretical study on the reduction mechanisms of CO dimer into $C_2H_4$. This present reduction pathway is consistent with the latest experimental results and explains the puzzle in experiment on uncertainty of reaction intermediates. At present, it seems to us that the mechanism that proposed in this work is most agreeable with the present experimental results.

**Keywords** CO Dimerization; $C_2H_4$; Cu(100); Reduction Mechanism; Kinetics

*College of Chemistry and Chemical Engineering, Hunan University of Arts and Science, Changde 415000, China.*
** To whom correspondence should be addressed. E-mail: oulihui666@126.com.*
*Phone: +86-736-7186115.*
Electronic supplementary information (ESI) available.

## 1. Introduction

Reducing carbon dioxide ($CO_2$) into carbon-neutral fuel and renewable feedstock of carbon-based fine chemicals would positively impact the global carbon balance and offer a novel solution to the dilemma of growing energy demand and global warming we are facing nowadays.[1, 2] In this area, a landmark discovery was made in 1985 by Hori, who found that $CO_2$ can be reduced to ethylene ($C_2H_4$) and methane ($CH_4$) on Cu electrodes,[3] and the extent of $C_2H_4$ and $CH_4$ formation sensitively depends on the surface orientation of the Cu electrode.[4] On the (100) facet of Cu fcc crystal, the formation of $C_2H_4$ is dominant, whereas on the (111) facet, the formation of $CH_4$ is favored. However, an overpotential of almost 1 V on Cu electrodes is required, which hinder global spread of this technology. Thus, the study of reduction mechanism of $CO_2$ is extremely urgent on Cu electrode. At present, most of the studies devoted to understanding its reduction mechanism on Cu electrodes have been experimental,[5-10] while theoretical insight has been provided recently for the formation of $C_1$ species, such as $CH_4$.[11-16] In spite of extensive literature, the molecular-level details of the mechanism of the $CO_2$ reduction on Cu electrodes is still not clearly understood, in particular in relation to the C-C coupling step leading to the formation of $C_2H_4$ on Cu(100). However, all of these studies showed that CO appears to be an important intermediate during the course of reduction. Electroreduction of CO leads to a similar product distribution as observed for $CO_2$ reduction,[17] producing both $C_2H_4$ and $CH_4$ through different reduction pathways. Similar hydrocarbon products yielded in experiments on CO electroreduction on Cu electrodes have established that adsorbed CO is a key intermediate in the formation of both $C_2H_4$ and $CH_4$.[17-19] Thus, the study of CO reduction mechanisms on copper electrodes will lead to a deeper understanding of the reaction chemistry and can eventually lead to the design of more efficient and selective catalysts, which can explain the observed product distribution and the effect of different electrode facets on catalytic activity and selectivity of reaction.

Recent experimental and theoretical studies to focus on the CO reduction mechanism have mostly showed that adsorbed CHO* is a key reaction intermediate and the hydrogenative reduction of CO to an adsorbed CHO* as the rate-determining step (rds), eventually resulting in the formation of $CH_4$ by successive hydrogenation of cleavage of the C-O bond on Cu electrodes.[5-16] However, the exact reduction mechanism of CO into $C_2H_4$ is still debated. The studies by Schouten and coworkers[8-10] have suggested that a mechanism may exist whose rds does not depend on a proton-coupled electron transfer from an experimental standpoint since they found that yields of $C_2$ species are pH dependent on an RHE scale in experiment. In order to explain this phenomenon, a CO dimerization mechanism in both $CO_2$ and CO electroeduction is proposed on Cu(100) by Schouten and coworkers, and the electroreduction of various potential intermediates to

hydrocarbons suggests that the dimerization of CO is the rate-determining step in $C_2$ species formation, followed by either the formation of an enediol-like species or an oxalometallocycle.[8] Further work by Schouten and coworkers demonstrates a shift in the onset of $C_2$ formation to potentials around -0.4 V vs. reversible hydrogen electrode (RHE), providing further evidence that CO dimerization may occur.[9] Li et al. and Kas et al. also suggest a C-C coupling mechanism based on the yields of $C_2H_4$ on oxide-derived Cu electrodes at potentials less negative than -0.5 V vs RHE.[20, 21] Previous theoretical studies performed by Montoya and coworkers have shown that kinetic barriers to the formation of a C-C bond between unprotonated CO adsorbates on Cu(211) surfaces are too high at a vacuum-metal interface for the turnover of production $C_2$ species at reasonable rates, the qualitative trends would not be changed even in the presence of applied electric fields likely to exist in electrochemical environments,[22] suggesting that CO* dimerization is kinetically unfavorable on Cu(211), and therefore of CO* to form CHO* intermediate must be proceeded before favorable kinetics can be achieved in the formation of $C_2H_4$. Calle-Vallejo and coworkers[23] showed that concerted proton-electron transfer, there is no impact of pH value on the formation of production $C_2H_4$ on Cu(100), suggesting that the rds happens at an early stage of the mechanism and that there should be no proton transfer involved in that step or in the one before it from the theoretical standpoint. Thus, it can be concluded that C-C coupling should happen before the first proton transfer for the lowest-overpotential reduction pathways. Simultaneously, their studies also suggested that activation energies to CO dimerization with an Eley-Rideal mechanism (i.e., only one of the CO molecules adsorbs on the surface and the other one from the gas phase reacts with the adsorbed CO molecule directly, without adsorbing), are not as high on Cu(100) compared with that with an Langmuir-Hinshelwood mechanism, i.e., two CO molecules adsorb at neighboring sites on Cu(111). However, the exergonic binding energy of CO on (211) steps and (100) terraces of Cu[15] suggest that adsorbed, rather than gas-phase CO is the relevant precursor to the kinetics of C-C coupling between two CO molecules. Additionally, this previous work from Calle-Vallejo and coworkers also proposed a stabilization of the CO dimer and its transition state by scaling the energy using the number of excess electrons in the adsorbed species as determined from a Bader charge analysis. Most recently, Montoya and coworkers presented DFT simulations for CO dimerization mechanism and demonstrated that CO dimerization should have a lower activation barrier on Cu(100) than Cu(111),[24] suggesting that Cu(100) surface has a high activity for C-C coupling. However, the theoretical study conducted by Montoya and coworkers only considered C-C coupling mechanism of Cu(211) surface,[22] whereas Cu(100) facet has been reported to be particularly selective towards $C_2H_4$ production. $C_2$ products can be formed at low overpotentials without the formation of $C_1$ products on Cu(100).[3, 4, 8, 9, 17-19] Although

they also considered CO dimer as the intermediate during the course of the formation of $C_2H_4$, no detailed DFT-based mechanism for the formation of $C_2H_4$ was suggested on Cu(100).[24] In the theoretical study on Cu(100) from Calle-Vallejo and coworkers, the used model is purely thermodynamically and assumes that the kinetic barriers of uphill processes are not much larger than their reaction energies and those downhill processes have easily surmountable barriers.[23] In spite of extensive experimental and theoretical studies, it is still unknown whether adsorbed CO or a more reduced $C_1$ species is coupled to make $C_2H_4$ production, thus leaving the main reaction path, reaction intermediates and selectivity-determining and rate-determining steps for $C_2H_4$ production on Cu(100) electrocatalysts still uncertain. Understanding the C-C bonding formation is important, as it would aid in the design of new catalysts that are active at a lower overpotential and open up routes to the production of high-energy fuels by the electrochemical reduction of $CO_2$.

In the present work, we carry out a systematic DFT study of reduction mechanism of CO dimer to form production $C_2H_4$ in $CO_2$ electroreduction on Cu(100) electrode, for the first time examining the kinetic energy of various possible elementary reaction steps during the course of reduction of CO dimer to form production $C_2H_4$, and determining the selectivity-determining and rate-determining steps. As electrocatalytic reactions on catalysts that include electrolyte environment are far too complex for a complete theoretical description into kinetics of elementary steps, the complexity is first reduced. Consequently, in the present study, we restrict our calculations to close packed surfaces and periodic gas-phase environment. However, the theoretical evidence of reduction mechanism of CO dimer of Cu(100) surface is still able to be presented qualitatively in this work. The results will explain the experimental observations and provide theoretical support for the reduction mechanism of CO dimer previously proposed by Schouten and coworkers.

## 2. Computational method and modeling

Calculations were performed in the framework of DFT using the generalized gradient approximation (GGA) of Perdew-Burke-Ernzerhof (PBE)[25] and employing ultrasoft pseudopotentials[26] for Nuclei and core electrons of all atoms. The calculations of the most stable geometry structure of various adsorption and co-adsorption intermediates were performed using periodic super-cells with the Cu electrodes modeled by four-layer (100) slabs with a 3×3 surface. A vacuum space of 16Å was placed above the slabs and adsorption is allowed on only one of the two surfaces exposed. The Kohn-Sham orbitals were expanded in a plane-wave basis set with a kinetic energy cutoff of 26 Ry and the charge-density cutoff of 260 Ry. The Fermi-surface effects was treated by the smearing technique of Methfessel and Paxton, using a smearing parameter[27] of 0.02 Ry. Calculations were carried out with spin-polarization, which is essential to properly represent the

electronic structure of adsorbed various reaction intermediates. The PWSCF codes contained in the Quantum ESPRESSO distribution[28] were used to implement all calculations, while figures of the chemical structures were produced with the XCRYSDEN[29-31] graphical package. BZ integrations were performed using a (3×3×1) uniformly shifted k-mesh for (3×3) supercell. The calculated equilibrium lattice constant for Cu was 3.66Å, which agreed well with theoretical and experimental values (3.66 and 3.62Å, respectively).[32, 33] During the calculations, the structure of the bottom two layers were fixed at the theoretical bulk positions, whereas the top two layers and the adsorbates were allowed to relax and all the other structural parameters were optimized so as to minimize the total energy of the system. Structural optimization was performed until the Cartesian force components acting on each atom were brought below $10^{-3}$ Ry/Bohr and the total energy converged to within $10^{-5}$ Ry.

The climbing-image nudged elastic band (CI-NEB) method was used to determine the minimum energy paths (MEPs) for all the elementary steps.[34, 35] The transition state of the optimized reaction coordinate was approximated by the image of highest energy. The transition state images from the CI-NEB calculations were optimized using the quasi-Newton method, which minimizes the forces to find the saddle point. Geometry optimization was performed for each intermediate point in MEPs, in which considering the high cost of CI-NEB calculations, the most stable adsorption configurations of adsorbents obtained on 3×3 surface and a three-layer Cu(100) slab with a 2×3 surface unit cell were used, the bottom two layers of metal atoms were fixed while the top layer of metal atoms and all other nonmetal atoms were allowed to relax.

**Fig. 1** Minimum energy path of on Cu(111) CO dissociation and hydrogenation to form C, COH and CHO, respectively. Oxygen atoms are red, hydrogen atoms are white, carbon atoms are gray, and copper atoms are blue.

## 3. Results

The adsorption, co-adsorption energies and geometry structures of preferred adsorption configurations for various possible reaction intermediates on Cu(100) are given in Tables S1, S2 and Figures S1, S2 in the Supporting Information (SI). The most stable adsorption configurations on Cu(100) are used to perform following MEP analysis. The hydrogenation agent in the elementary reaction steps of reduction mechanism of CO dimer is the adsorbed hydrogen atoms (H*) formed through $H_2$ dissociation. A Langmuir-Hinshelwood mechanism is involved in reduction mechanism of CO dimer since the adsorbents are co-adsorbed structures on Cu(100). The DFT-calculated activation barrier for $H_2$ dissociation is 0.45 eV

on Cu(100), which are small and easily to be surmountable. Therefore, the $H_2$ dissociation should play a relatively minor role in the kinetics of reduction mechanism of CO dimer.

**Fig. 2** Minimum energy path of CO dissociation and hydrogenation on Cu(100) to form C, COH and CHO, respectively.

**3.1 Selectivity-determining steps of CO reduction on Cu(111) and Cu(100)**

The studies conducted by Schouten and coworkers[8] suggested that there are two separate pathways for the formation of $C_2H_4$, one that shares an intermediate with the pathway to $CH_4$, as observed on Cu(111) and below -0.8 V on the Cu(100) surface at pH 7, and a second pathway that occurs only on the Cu(100) surface. Our recent theoretical study[16] had reported the formation pathways of $CH_4$ and $C_2H_4$ by the chemical and electrochemical reduction of $CO_2$ on Cu(111) and Cu(100) that sharing key intermediates $CO_{ads}$, $CHO_{ads}$, $CH_2O_{ads}$ and $CH_2OH_{ads}$. The key intermediate $CH_{2ads}$ can be formed by hydrogenative dissociation of the $CH_2OH_{ads}$ intermediate, finally, the $CH_2$ intermediate leads to formation of the $CH_4$ and $C_2H_4$ by serial hydrogenation and dimerization, respectively. For this second pathway, they suggest that the CO dimer, OCCO* is the key intermediate in the formation of $C_2H_4$. So far, it is still unclear about selectivity-determining steps, namely, CO hydrogenation or CO dimerization is more favorable on Cu(111) and Cu(100). Therefore, the MEP analysis for CO further reduction is performed in this section to ascertain the selectivity-determining steps. On Cu(111) and Cu(100), there are two possible reactions for the CO further hydrogenation, namely, the hydrogenation to form an adsorbed formyl (CHO*) and hydroxymethylidyne (COH*). Additionally, the direct dissociation to adsorbed C* and O* is also considered. The calculated MEPs (Fig. 1 and 2) suggest that the direct dissociation is particularly energetically demanding, the activation barrier is 3.96 and 3.01 eV on Cu(111) and Cu(100), respectively. The two hydrogenation reactions have relatively lower activation barriers, and the formation of CHO* requires an activation barrier nearly 1.6 eV lower than the formation COH* (~1.0 eV vs ~2.6 eV) on Cu(111). The activation energy barriers for the hydrogenation of CO to form COH* and CHO* required is 2.43 and 2.36 eV on Cu(100), respectively, as shown in Fig. 2. These results indicated that CO hydrogenation requires higher activation energy barriers on Cu(100) than that on Cu(111), which is more easily to achieve on Cu(111). On this basis, it may be able to be concluded that CO further hydrogenation to CHO* is more favorable on Cu(111).

As shown in Fig. 3 and 4, the activation energy barrier for the formation of OCCO* intermediate by CO dimerization on Cu(111) and Cu(100) is 1.59 and 1.26 eV, respectively. Our present results indicated that CO

dimerization into OCCO* intermediate requires higher activation energy barrier than CO hydrogenation into CHO* intermediate on Cu(111), whereas on Cu(100), lower activation energy barrier is required for CO dimerization compared to the formation of CHO* intermediate by CO hydrogenation. Therefore, CO hydrogenation into CHO* during the course of CO further reduction is more easily to occur on Cu(111), whereas CO dimerization into OCCO* is more favorable on Cu(100). A relation between the surface structure of the Cu electrodes and the mechanism of CO reduction is suggested by our present theoretical study, and selectivity-determining steps are revealed on these both different Cu single-crystal electrode surface. The previous experiment study by Hori *et al*.[3, 4, 17-19] on Cu single electrode surfaces and thermodynamic and kinetic theoretical study conducted by Calle-Vallejo *et al*. and Nørskov *et al*.[23, 36] also showed that on Cu(100) more $C_2H_4$ is formed whereas on Cu(111) more $CH_4$ is produced. Therefore, we can speculate that the formation of $CH_4$ is more favorable on atomically flat (111) parts of the Cu electrode surface through CO hydrogenation into CHO* intermediate, whereas $C_2H_4$ will be more easily to be formed at (100) sites by CO dimerization. Simultaneously, the previous DFT calculations from Peterson *et al*. and Nie *et al*.[11, 14] also suggested that CHO* is the intermediate in the formation of $CH_4$, and no any experimental evidence indicated that CHO* is the precursor to $C_2H_4$.[8, 9] A second key aspect of our present result is that the activation energy barrier for CO dimerization on Cu(100) facet is significantly lower than that on Cu(111) facet. The structure sensitively described by the lowering of the activation energy barrier on Cu(100) relative to Cu(111) implies that Cu(100) facet has more activity for reduction mechanism of CO dimer as indicated in previous experimental studies. Thus, the unique selectivity for the formation of $C_2H_4$ on (100) can be explained by reduction mechanism of CO dimer (for detailed arguments, see ref 37) and is consistent with the suggestion of Gattrell and coworkers[38] who proposed that this CO dimer would be more stable on Cu(100). Additionally, our present results are also in agreement with Schouten and coworkers' experimental study. Currently, the mechanism of $C_2H_4$ formation initiated by CO dimerization is studied in more detail on Cu(100) for the first time from the point of view of kinetics in our present study as follows.

**Fig. 3** Minimum energy paths of CO dimerization into OCCO* intermediate on Cu(111).

**Fig. 4** Minimum energy paths of CO dimerization into OCCO* intermediate on Cu(100).

### 3.2 The Serial Reduction Pathways of CO Dimer into $C_2H_4$ on Cu(100)

To find intermediates in the reduction of CO dimer, OCCO* into production $C_2H_4$, we investigated the

reduction of $C_2$ species. The kinetic energetics of OCCO* intermediate further hydrogenation or dissociation are firstly examined on Cu(100). There are three possibilities for further reduction of OCCO* intermediate. One is dissociation of OCCO* by breaking of C-O bond to form CCO* intermediate; the other two are hydrogenation of OCCO* at C and O atom site to form OCCHO* and OCCOH* intermediates, respectively. In order to compare the degree of difficulty of these two possibilities, the minimum energy path (MEP) analysis was performed. As shown in Fig. 5, the activation barriers for the dissociation of OCCO* into CCO* is 0.91 eV, and further hydrogenation of OCCO* into OCCHO* and OCCOH* on Cu(100) are 0.21 and 1.16 eV, respectively, in which the activation barrier of hydrogenation of OCCO* on C atom site is significantly lower and can be easily overcome at ambient temperature. Although recent theoretical study conducted by Calle-Vallejo and coworkers[23] based on thermodynamics analysis suggested that CCO* is possible reaction intermediate in the electroreduction of CO to $C_2$ species on Cu(100), the cleavage of C-O bond in OCCO* is unfavorable kinetically on Cu(100). Therefore, it can be concluded that the further reduction of OCCO* into OCCHO* intermediate should be more kinetically favorable on Cu(100).

**Fig. 5** Minimum energy paths of OCCO* hydrogenation into OCCHO* and OCCOH*, and dissociation into CCO* by cleavage of C-O bond on Cu(100), respectively.

For further reduction of OCCHO* intermediate, there may be three possibilities on Cu(100). One is hydrogenation of OCCHO* at C atom site into glyoxal (OHCCHO*); the other two is hydrogenation of OCCHO* at O atom site into HOCCHO* and OCCHOH* intermediate, respectively. As shown in Fig. 6, the activation barriers for the further hydrogenation of OCCHO* into OHCCHO*, HOCCHO* and OCCHOH* intermediate on Cu(100) based on the MEP analysis are 0.09, 0.22, and 0.62 eV, respectively, in which the formation of OHCCHO* intermediate requires significantly lower activation energy, and which is almost a non-activated process. Therefore, the hydrogenation of OCCHO* into OHCCHO* intermediate at C atom site is more easily to occur on Cu(100). Our present theoretical calculations are also agreeable with recent experimental study by Schouten and coworkers,[8] in which OHCCHO* intermediate had been observed experimentally as a reaction intermediate during the course of CO reduction on Cu(100).

**Fig. 6** Minimum energy paths of OCCHO* intermediate hydrogenation into OCCHOH*, HOCCHO* and OHCCHO* on Cu(100), respectively.

**Fig. 7** Minimum energy paths of further reduction of OHCCHO* intermediate into $OHCCH_2O$*,

OHCCHOH* and OHCCH* on Cu(100), respectively.

Similarity, three possibilities are also considered for further reduction of OHCCHO* intermediate. One is deoxygenation of OHCCHO* intermediate to form adsorbed OHCCH* and O* atom by cleavage of C-O bond; the other two is hydrogenation of OHCCHO* at C and O atom site to form $OCHCH_2O$* and OHCCHOH* intermediate, respectively. The MEP analysis indicated that the activation barriers for deoxygenation of OHCCHO* into OHCCH* and O* atom is 1.02 eV and the activation barriers for the further hydrogenation of OHCCHO* into $OHCCH_2O$ and OHCCHOH* on Cu(100) are 0.63 and 1.23 eV, respectively, see Fig. 7. The hydrogenation of OHCCHO* at C atom site into $OHCCH_2O$* has relatively lower activation barrier on Cu(100). Therefore, the formation of $OHCCH_2O$ is the most favorable kinetically reaction pathway on Cu(100) for the further reduction of OHCCHO* intermediate.

Based on above analysis, we can speculate that OHCCHO* and $OHCCH_2O$* are possible reaction intermediates in reduction mechanism of CO dimer on Cu(100). There are also three possibilities for further reduction of $OHCCH_2O$*. One is hydrogenation of $OHCCH_2O$* at C atom site in CHO part into $OH_2CCH_2O$* intermediate; the other two is hydrogenation of $OHCCH_2O$* at O atom site in $CH_2O$ and CHO part into $OHCCH_2OH$* and $HOHCCH_2O$* intermediate, respectively. For these three possibilities, the MEP analysis was also performed. As shown in Fig. 8, the activation barriers for the further reduction of $OHCCH_2O$* intermediate into $OH_2CCH_2O$*, $OHCCH_2OH$* and $HOHCCH_2O$* on Cu(100) are 0.38, 0.98 and 0.78 eV, respectively, in which the formation of $OH_2CCH_2O$* has relatively lower activation barrier on Cu(100). Therefore, it can be predicted that $OH_2CCH_2O$* should be the most kinetically favorable state derived from the hydrogenation of $OHCCH_2O$* at C atom site in CHO part on Cu(100).

**Fig. 8** Minimum energy paths of further hydrogenation of $OHCCH_2O$* intermediate into $OH_2CCH_2O$*, $OHCCH_2OH$* and $HOHCCH_2O$* on Cu(100), respectively.

For further reduction of $OH_2CCH_2O$* intermediate, there may be two possibilities. One is hydrogenation of $OH_2CCH_2O$* at O atom site into $OH_2CCH_2OH$* intermediate; another is deoxygenation of $OH_2CCH_2O$* to form $OH_2CCH_2$* intermediate by cleavage of C-O bond. The MEP analysis of these two possibilities was performed for comparison. As shown in Fig. 9, the activation barriers for the hydrogenation of $OH_2CCH_2O$* into $OH_2CCH_2OH$* intermediate and deoxygenation into $OH_2CCH_2$* on Cu(100) are 1.21 and 2.71 eV, respectively. By comparing the activation barriers, the formation of $OH_2CCH_2OH$* has relatively lower barrier, and it is significantly lower than that of the formation of $OH_2CCH_2$*. Therefore, we can conclude that $OH_2CCH_2OH$* should be more kinetically favorable intermediate derived from the

hydrogenation of $OH_2CCH_2O$* intermediate other than $OH_2CCH_2$* intermediate formed by cleavage of C-O bond in $OH_2CCH_2O$*.

**Fig. 9** Minimum energy paths of further reduction of $OH_2CCH_2O$* intermediate into $OH_2CCH_2OH$* by hydrogenation and $OH_2CCH_2$* on Cu(100) by cleavage of C-O bond, respectively.

**Fig. 10** Minimum energy paths of further reduction of $OH_2CCH_2OH$* intermediate into $HOH_2CCH_2OH$* by hydrogenation and $OH_2CCH_2$* by dehydroxylation and $H_2CCH_2OH$* by deoxygenation on Cu(100), respectively.

Three possibilities are considered for further reduction of $OH_2CCH_2OH$* intermediate. One is hydrogenation of $OH_2CCH_2OH$* at O atom site in $CH_2O$ part to form $HOH_2CCH_2OH$* intermediate; the other two is dehydroxylation and deoxygenation of $OH_2CCH_2OH$* to form $OH_2CCH_2$* and $H_2CCH_2OH$* intermediate, respectively. The MEP analysis for these three possibilities showed that the activation barriers for the further hydrogenation of $OH_2CCH_2OH$* into $HOH_2CCH_2OH$*, and dehydroxylation and deoxygenation of $OH_2CCH_2OH$* to $OH_2CCH_2$* and $H_2CCH_2OH$* on Cu(100) are 1.21, 1.36 and 1.12 eV, respectively, see Fig. 10. It can be found that the hydrogenation of $OH_2CCH_2OH$* into $HOH_2CCH_2OH$* intermediate and deoxygenation of $OH_2CCH_2OH$* to $H_2CCH_2OH$* intermediate have almost identical and relatively lower activation barriers on Cu(100), indicating that these two pathways may be parallel, and may occur simultaneously during the course of $C_2H_4$ formation.

**Fig. 11** Minimum energy paths of further reduction of $HOH_2CCH_2OH$* and $H_2CCH_2OH$* intermediates into $C_2H_4$ by dehydroxylation on Cu(100), respectively.

$HOH_2CCH_2OH$* and $H_2CCH_2OH$* intermediates may be formed simultaneously on Cu(100) based on above analysis. Therefore, the final product $C_2H_4$ will be formed possibly by dehydroxylation of $HOH_2CCH_2OH$* and $H_2CCH_2OH$* intermediates. For these two possibilities, the MEP analysis indicated that the activation barriers for the dehydroxylation of $HOH_2CCH_2OH$* and $H_2CCH_2OH$* intermediates into $C_2H_4$ on Cu(100) are 0.45 and 0.28 eV, respectively, as shown in Fig. 11, The results showed that dehydroxylation of $H_2CCH_2OH$* into final product $C_2H_4$ have relatively lower activation barrier on Cu(100), indicating that the reaction may be more easily to occur on Cu(100). However, the activation barriers of the dehydroxylation of $HOH_2CCH_2OH$* into production $C_2H_4$ is also very low, which is also surmountable at ambient temperature. Therefore, these two pathways may occur simultaneously on Cu(100).

**Table 1** The optimal reduction pathways for CO dimerization into production $C_2H_4$ and the activation barriers ($E_{act}$) of each elementary reaction step on Cu(100).

| Reaction Paths | $E_{act}$ (eV) |
|---|---|
| (CO + CO)* → OCCO* | 1.26 |
| (OCCO + H)* → OCCHO* | 0.21 |
| (OCCHO + H)* → OHCCHO* | 0.09 |
| (OHCCHO + H)* → $OHCCH_2O$* | 0.63 |
| ($OHCCH_2O$ + H)* → $OH_2CCH_2O$* | 0.38 |
| ($OH_2CCH_2O$ + H)* → $OH_2CCH_2OH$* | 1.21 |
| ($OH_2CCH_2OH$ + H)* → $HOH_2CCH_2OH$* | 1.21 |
| $OH_2CCH_2OH$* → ($H_2CCH_2OH$ + O)* | 1.12 |
| $HOH_2CCH_2OH$* + * → $H_2CCH_2$ + 2OH* | 0.45 |
| $H_2CCH_2OH$* → $H_2CCH_2$ + OH* | 0.28 |

## 4. Discussion

In the present study, a systematic determination of the CO reduction mechanism into production $C_2H_4$ is presented by CO dimerization on Cu(100), including the selectivity-determining steps, the optimal reduction pathways and rate-determining steps. We present the first DFT study that examines the role of kinetics of elementary reaction steps in reduction mechanism of CO dimer into production $C_2H_4$ on Cu(100), utilizing the MEP analysis. Based on above results from MEP analysis, the optimal reaction pathways by CO dimerization into production $C_2H_4$ on Cu(100) can be summarized in Table 1. CO dimer, OCCO* is firstly formed by CO dimerization, and this reaction is more favorable on Cu(100) than the further hydrogenation of CO. Based on the activation barriers, the $OH_2CCH_2OH$* intermediate either forms $HOH_2CCH_2OH$* intermediate by direct hydrogenation or forms $H_2CCH_2OH$* intermediate by cleavage of C-O bond, which maybe parallel pathways in reduction mechanism of CO dimer on Cu(100). Finally, the production $C_2H_4$ can be formed by dehydroxylation of $HOH_2CCH_2OH$* and $H_2CCH_2OH$* intermediates. Based on the calculated activation barriers, the relatively slow steps on Cu(100) include (CO + CO)* → OCCO*, ($OH_2CCH_2O$ + H)* → $OH_2CCH_2OH$*, ($OH_2CCH_2OH$ + H)* → $HOH_2CCH_2OH$*, and $OH_2CCH_2OH$* → ($H_2CCH_2OH$ + O)*, in which (CO + CO)* → OCCO* has the highest activation barrier, and it may be rate-determining step of reduction mechanism of CO dimer into $C_2H_4$ on Cu(100). Our present mechanistic study explain the experimental observations by Schouten and coworkers that a rate-determining step consist of the coupling of

two CO molecules mediated by electron transfer to form OCCO* intermediate on Cu(100). Simutaneously, it can be found that the coupling of C-C bond, hydrogenation at O atom site, and cleavage of C-O bond is more difficult to occur on Cu(100) for CO reduction into production $C_2H_4$. The possible reduction mechanism of CO dimer into $C_2H_4$ is proposed in Fig. 12 based on our DFT calculated results on Cu(100).

**Fig. 12** Proposed reduction pathways into production $C_2H_4$ in reduction mechanism of CO dimer on Cu(100).

In the previous mechanistic study on CO reduction into $C_2H_4$, the combination of two adsorbed $CH_2$* species and a CO-insertion type mechanism, namely, a coupling between $CH_x$ and CO leading to the formation of $CH_xCO$ species, were proposed by Hori and coworkers[3, 4, 17-19, 37] as alternative pathways for the formation of production $C_2H_4$, but such these two mechanisms cannot explain why main C-C coupling product $C_2H_4$ is observed experimentally on Cu(100). From thermodynamic view of point, recent theoretical considerations on the reduction of CO by dimerization to production $C_2H_4$ on Cu(100) electrode were performed by Calle-Vallejo and coworkers, and the possible reduction pathways were proposed. Based on the thermodynamic study, OCCHO* intermediate is less stable than OCCOH* intermediate, suggesting that an initial hydrogenation of the O atom in OCCO* intermediate is a more favorable pathway on Cu(100), and then CCO* intermediate was formed by dehydroxylation of OCCOH* intermediate (i.e. the cleavage of C-O bond). The next favorable step is a hydrogenation of CCO* at C atom site to form HCCO* intermediate, followed by a hydrogenation of HCCO* in the carbonyl group into HCCHO* intermediate. In the next step another hydrogenation takes place at C atom site of HCCHO*, producing $H_2CCHO$* intermediate. The further reduction pathway of $H_2CCHO$* proceeds with the hydrogenation of the C atom bonded to the O atom, leading to formation of $H_2CCH_2O$* intermediate. Finally, the production $C_2H_4$ was formed by cleavage of C-O bond on Cu(100). Therefore, previous thermodynamic studies showed that CCO*, HCCO*, HCCHO*, $H_2CCHO$*, and $H_2CCH_2O$ are intermediates of reduction mechanism of CO dimer. However, our present mechanistic studies showed that the initial hydrogenation of OCCO* at C atom site into OCCHO* should be more a favorable pathway on Cu(100) other than forming OCCOH* intermediate by the hydrogenation of O atom, the corresponding activation barriers are 0.21 and 1.16 eV. The OCCHO*, OHCCHO*, $OHCCH_2O$*, $OH_2CCH_2O$*, $OH_2CCH_2OH$*, $HOH_2CCH_2OH$*, and $H_2CCH_2OH$* are key reduction intermediates in reduction mechanism of CO dimer on Cu(100), which are not in agreement with the previous thermodynamic study. Furthermore, the formation of HCCHO* is relatively more difficult during the course of further reduction of OHCCHO*, which is not a kinetically favorable pathway, and an activation barrier of 1.02 eV is required by deoxygenation of OHCCHO* (i.e. the cleavage of C-O bond). In

our present mechanistic study, $H_2CCH_2O$* intermediate can be formed by deoxygenation of $OH_2CCH_2O$* and dehydroxylation of $OH_2CCH_2OH$*. However, the activation barriers of $H_2CCH_2O$* formation in these two pathways are very high (2.71 and 1.36 eV, respectively) compared to further hydrogenation of $OH_2CCH_2O$* and $OH_2CCH_2OH$*. Therefore, the formation of $H_2CCH_2O$* intermediate may be not kinetically favorable step during the course of CO reduction by dimerization. Considering the difficulty of cleavage of C-O bond, we can infer that $H_2CCHO$* is not also reduction intermediate in reduction mechanism of CO dimer. The present mechanistic study results show that the preferred pathway on Cu(100) solely based on reaction free energies may be misleading, and reaction kinetics of elementary reaction steps provide a different mechanistic explanation for selectivity of production $C_2H_4$ compared to $CH_4$ on Cu electrodes. An alternative reaction pathway that suggests production $C_2H_4$ through OCCO* intermediate from CO dimerization is provided in our present mechanistic study. This reduction pathway is consistent with the latest experimental results and explains the puzzle in experiment from Schouten and coworkers,[8, 9] who suggested that OHCCHO*, HOCCOH*, and $H_2CCH_2O$* are possible reduction intermediates in reduction mechanism of CO dimer into $C_2H_4$, but still uncertain. Our present research results provide an explanation that OHCCHO* is a key reaction intermediate in reduction mechanism of CO dimer other than HOCCOH* and $H_2CCH_2O$* on Cu(100). At present, it seems to us that the mechanism proposed in Fig. 12 is most agreeable with the experimental results. In reality, electrode potential should be considered in our present MEP analysis. However, the kinetic model that coupling with electrode potential still need to be further explored in the future because of the uncertainty of the electrode potential, in which the work function differs among these adsorbed states when kinetically modeling electrochemical reaction systems, leading to differences in electrode potentials during the reaction. Although the relationship between the kinetic electrochemical reduction pathways of CO and electrode potential from our present data cannot be deduced, the conclusions in trends are expected to be reasonably accurate.

**5. Conclusions**

A systematic DFT study that examines the role of kinetics of elementary steps in reduction mechanism of CO dimer into production $C_2H_4$ on Cu(100) is presented for the first time in the present work, and a new reduction mechanism is introduced. The kinetic analysis of elementary reaction steps have suggested that further reduction of CO is key selectivity-determining step for the formation of production $C_2H_4$ and $CH_4$ on Cu(100) and Cu(111). The main reaction pathway on Cu(111) proceeds through reduction of CO into CHO* intermediate, which may eventually result in $CH_x$ species by the breaking of C-O bond, and produce

production $CH_4$. On Cu(100), CO dimer, OCCO* is firstly formed by CO dimerization, which is the first step and more favorable pathway than the further hydrogenation of CO. It explains why only $C_2$ species and not $C_1$ species are observed experimentally on Cu(100). For the formation of production $C_2H_4$ on Cu(100), the results suggest that hydrogenation of OCCO* to OCCHO* intermediate is the most possible reaction path, followed by the formation of OHCCHO* intermediate through OCCHO* intermediate further hydrogenation. $OH_2CCH_2OH$* intermediate is formed by serial hydrogenation of OHCCHO*. The $OH_2CCH_2OH$* intermediate can form $HOH_2CCH_2OH$* by direct hydrogenation and $H_2CCH_2OH$* by breaking of C-O bond, which maybe a parallel pathway in reduction mechanism of CO dimer on Cu(100). Finally, the production $C_2H_4$ is formed by dehydroxylation of $HOH_2CCH_2OH$* and $H_2CCH_2OH$* intermediates. The formation of dimer, OCCO* may be rate-determining step in reduction mechanism of CO dimer on Cu(100). In contrast to previous suggested thermodynamic theoretical study on reduction mechanisms of CO dimer into production $C_2H_4$, our present reaction kinetics of elementary steps give a different mechanistic explanation for selectivity of production $C_2H_4$. This reduction pathway is consistent with the latest experimental results and explains the puzzle in experiment on uncertainty of reaction intermediates. Our present research results also provide an explanation that OHCCHO* is a key reaction intermediate in reduction mechanism of CO dimer on Cu(100) other than HOCCOH* and $H_2CCH_2O$* suggested in previous thermodynamic study. At present, it seems to us that the mechanism that proposed in this work is most agreeable with the present experimental results.

**Acknowledgements**

This work is financially supported by the National Natural Science Foundation of China (Grant No. 21303048), Hunan Provincial Natural Science Foundation of China (Grant No. 13JJ4101), the Construct Program of the Key Discipline in Hunan Province (Applied Chemistry) and Doctoral Start-up Fund of Hunan University of Arts and Science.

**References**

1 F. Hasegawa, S. H. Yokoyama and K. Imou, *Bioresource Techno*., 2010, **101**, S109−S111.

2 M. Abu-zahra, L. H. Schneiders, J. P. M. Niederer, P. H. Feron and G. F. Versteeg, *Int. J. Greenh. Gas con*., 2007, **1**, 37−46.

3 Y. Hori, K. Kikuchi and S. Suzuki, *Chem. Lett*., 1985, **14**, 1695−1698.

4 Y. Hori, I. Takahashi, O. Koga and N. Hoshi, *J. Mol. Catal. A: Chem*., 2003, **199**, 39−47.

5 W. Tang, A. A. Peterson, A. S. Varela, Z. P. Varela, Z. P. Jovanov, L. Bech, W. J. Durand, S. Dahl, J. K. Nørskov and I. Chorkendorff, *Phys. Chem. Chem. Phys*., 2012, **14**, 76−81.

6 K. P. Kuhl, E. R. Cave, D. N. Abram and T. F. Jaramillo, *Energy Environ. Sci*., 2012, **5**, 7050−7059.

7 K. P. Kuhl, T. Hatsukade, E. R. Cave, D. N. Abram, J. Kibsgaard and T. F. Jaramillo, *J. Am. Chem. Soc*., 2014, **136**, 14107−14113.

8 K. J. P. Schouten, Y. Kwon, C. J. M. van der Ham, Z. Qin and M. T. M. Koper, *Chem. Sci*., 2011, **2**, 1902−1909.

9 K. J. P. Schouten, Z. Qin, E. P. Gallent and M. T. M. Koper, *J. Am. Chem. Soc*., 2012, **134**, 9864−9867.

10 K. J. P. Schouten, E. P. Gallent and M. T. M. Koper, *ACS Catal*., 2013, **3**, 1292−1295.

11 X. Nie, M. R. Esopi, M. J. Janik and A. Asthagiri, *Angew. Chem. Int. Ed*., 2013, **52**, 2459−2462.

12 A. A. Peterson and J. K. Nørskov, *J. Phys. Chem. Lett*., 2012, **3**, 251−258.

13 P. Hirunsit, W. Soodsawang and J. Limtrakul, *J. Phys. Chem. C*, 2015, **119**, 8238−8249.

14 A. A. Peterson, F. Abild-Pederson, F. Studt, J. Rossmeisl and J. K. Nørskov, *Energy Environ. Sci*., 2010, **3**, 1311−1315.

15 W. J. Durand, A. A. Peterson, F. Studt, F. Abild-Pederson and J. K. Nørskov, *Surf. Sci*., 2011, **605**, 1354−1359.

16 L. H. Ou, *RSC Adv*., 2015, **5**, 57361−57371.

17 Y. Hori, R. Takahashi, Y. Yoshinami and A. Murata, *J. Phys. Chem. B*, 1997, **101**, 7075−7081.

18 Y. Hori, A. Murata, R. Takahashi and S. Suzuki, *J. Am. Chem. Soc*., 1987, **109**, 5022−5023.

19 Y. Hori, A. Murata, T. Tsukamoto, H. Wakebe, O. Koga and H. Yamazaki, *Electrochim. Acta*, 1994, **39**, 2495−2500.

20 C. W. Li, J. Ciston and M. W. Kanan, *Nature*, 2014, **508**, 504−507.

21 R. Kas, R. Kortlever, A. Milbrat, M. T. M. Koper, G. Mul and J. Baltrusaitis, *Phys. Chem. Chem. Phys*., 2014, **16**, 12194−12201.

22 J. H. Montoya, A. A. Peterson and J. K. Nørskov, *ChemCatChem*, 2013, **5**, 737−742.

23 F. Calle-Vallejo and M. T. M. Koper, *Angew. Chem. Int. Ed*., 2013, **52**, 7282−7285.

24 J. H. Montoya, C. Shi, K. Chan and J. K. Nørskov, *J. Phys. Chem. Lett*., 2015, **6**, 2032−2037.

25 J. P. Perdew, K. Burke and M. Ernzerhof, *Phys. Rev. Lett*., 1996, **77**, 3865−3868.

26 D. Vanderbilt, *Phys. Rev. B*, 1990, **41**, 7892−7895.

27 M. Methfessel and A. T. Paxton, *Phys. Rev. B*, 1989, **40**, 3616−3621.

28 S. Baroni, A. Dal Corso, S. de Gironcoli and P. Giannozzi, PWSCF and PHONON: Plane-Wave

Pseudo-Potential Codes. http://www.pwscf.org, 2001.

29 A. Kokalj, *J. Mol. Graph. Model*., 1999, **17**, 176−179.

30 A. Kokalj and M. Causà, *Scientific Visualization in Computational Quantum Chemistry*. *In Proceedings of High Performance Graphics Systems and Applications European Workshop*, CINECA-Interuniversity Consortium, Bologna, Italy, 2000.

31 A. Kokalj and M. Causà, XCrySDen: *X*-Window *CRY*stalline *S*tructures and *DEN*sities. http://www.xcrysden.org/, 2001.

32 J. Greeley, A. A. Gokhale, J. Kreuser, J. A. Dumesic, H. Topsøe, N. Y. Topsøe and M. Mavrikakis, *J. Catal*., 2003, **213**, 63−72.

33 *CRC Handbook of Chemistry and Physics*, 91st edition (Internet Version 2011), CRC Press/Taylor and Francis, Boca Raton, FL, 2011.

34 G. Henkelman and H. Jonsson, *J. Chem. Phys*., 2000, **113**, 9978−9985.

35 G. Henkelman, B. P. Uberuaga and H. Jonsson, *J. Chem. Phys.* 2000, **113**, 9901−9904.

36 J. H. Montoya, C. Shi, K. Chan and J. K. Nørskov, *J. Phys. Chem. Lett*., 2015, **6**, 2032−2037.

37 Y. Hori, K. Kikuchi, A. Murata and S. Suzuki, *Chem. Lett*., 1986, **15**, 897−898.

38 M. Gattrell, N. Gupta and A. Co, *J. Electroanal. Chem*., 2006, **594**, 1−19.

# A New Reduction Mechanism of CO Dimer by Hydrogenation into $C_2H_4$ on Cu(100) Surface: A Theoretical Insight into Kinetics of Elementary Steps

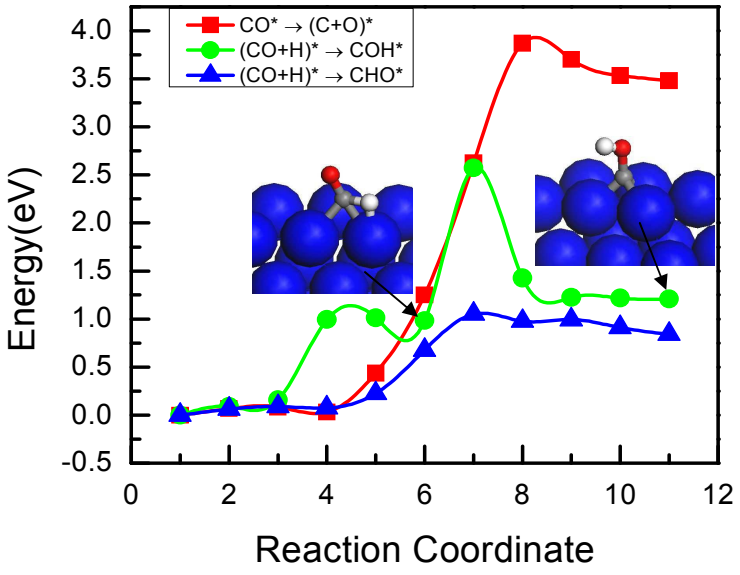


**Fig. 1** Minimum energy path of on Cu(111) CO dissociation and hydrogenation to form C, COH and CHO, respectively. Oxygen atoms are red, hydrogen atoms are white, carbon atoms are gray, and copper atoms are blue.

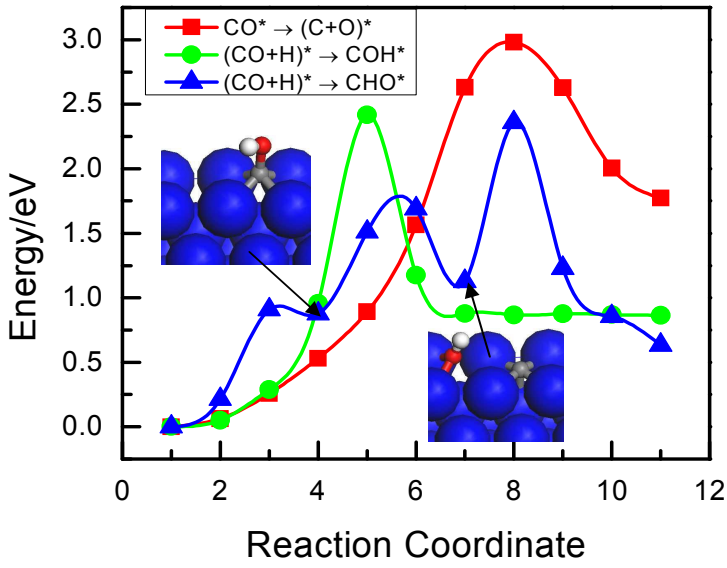


**Fig. 2** Minimum energy path of CO dissociation and hydrogenation on Cu(100) to form C, COH and CHO, respectively.

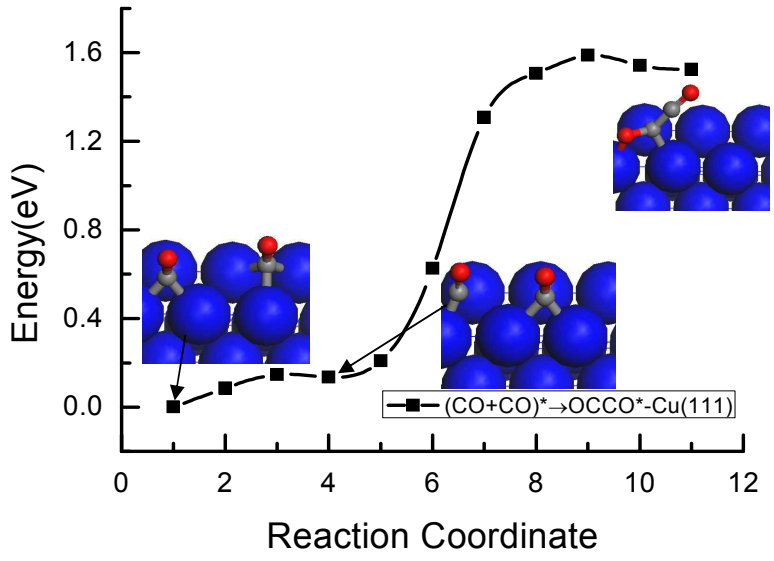


**Fig. 3** Minimum energy paths of CO dimerization into OCCO* intermediate on Cu(111).

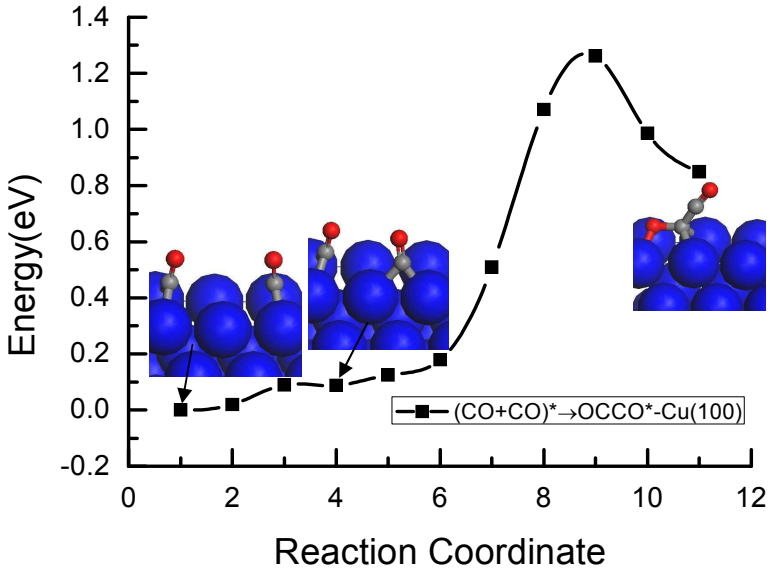


**Fig. 4** Minimum energy paths of CO dimerization into OCCO* intermediate on Cu(100).

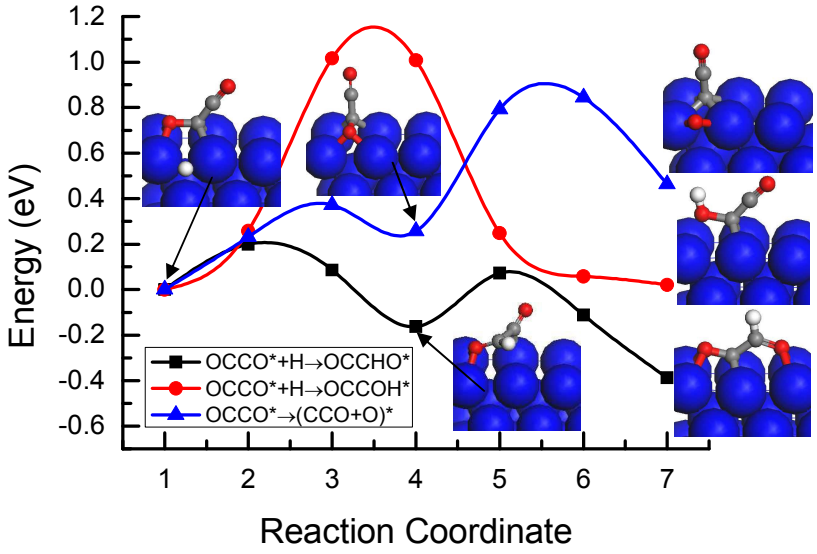


**Fig. 5** Minimum energy paths of OCCO* hydrogenation into OCCHO* and OCCOH*, and dissociation into CCO* by cleavage of C-O bond on Cu(100), respectively.

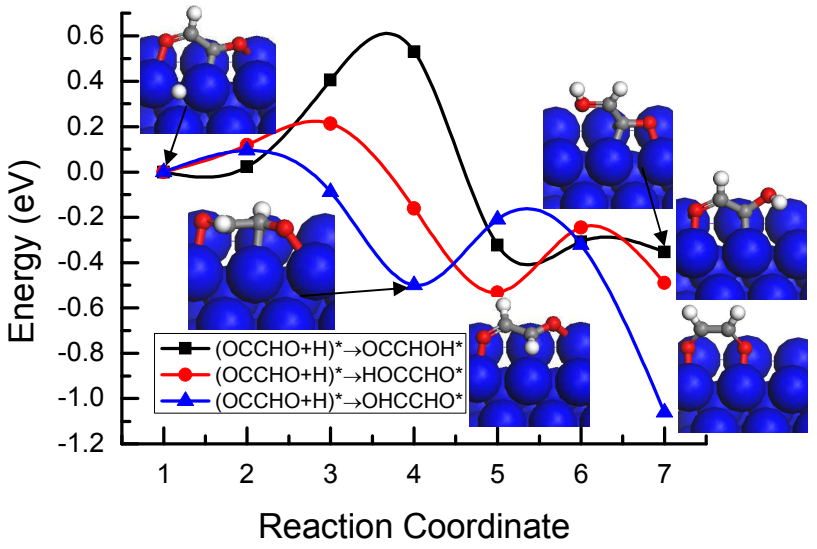


**Fig. 6** Minimum energy paths of OCCHO* intermediate hydrogenation into OCCHOH*, HOCCHO* and OHCCHO* on Cu(100), respectively.

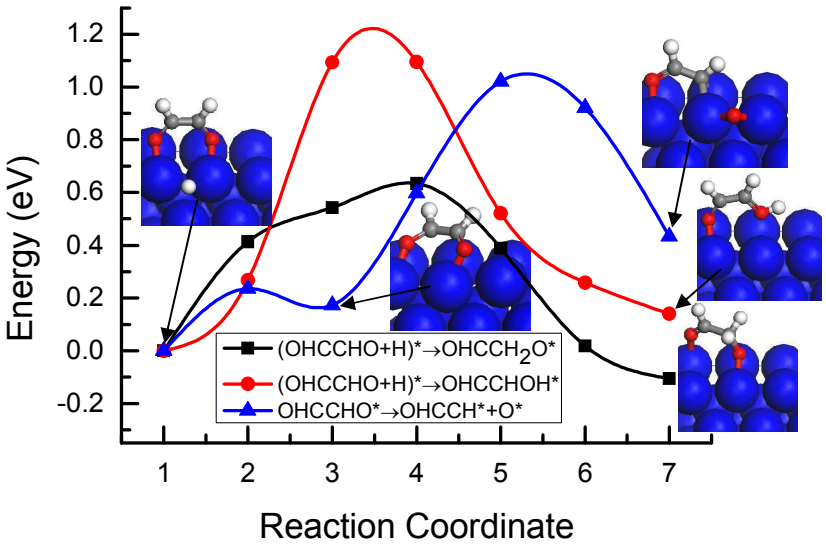


**Fig. 7** Minimum energy paths of further reduction of OHCCHO* intermediate into $OHCCH_2O$*, OHCCHOH* and OHCCH* on Cu(100), respectively.

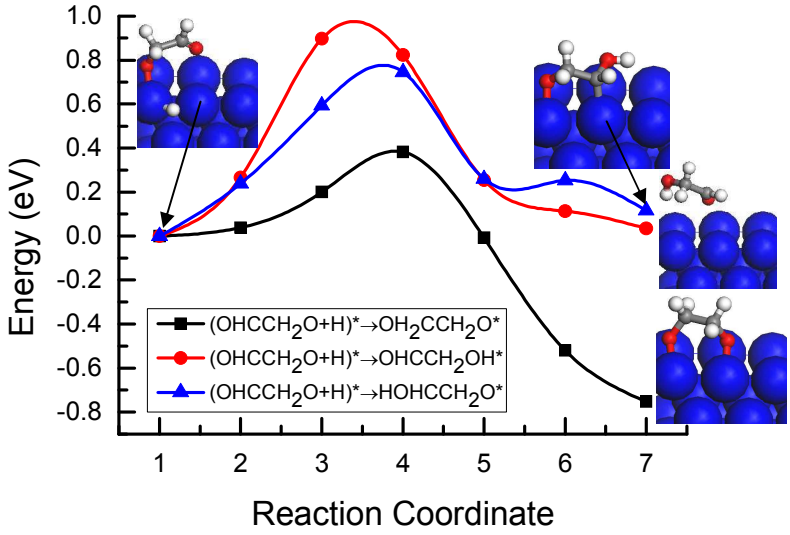


**Fig. 8** Minimum energy paths of further hydrogenation of $OHCCH_2O$* intermediate into $OH_2CCH_2O$*, $OHCCH_2OH$* and $HOHCCH_2O$* on Cu(100), respectively.

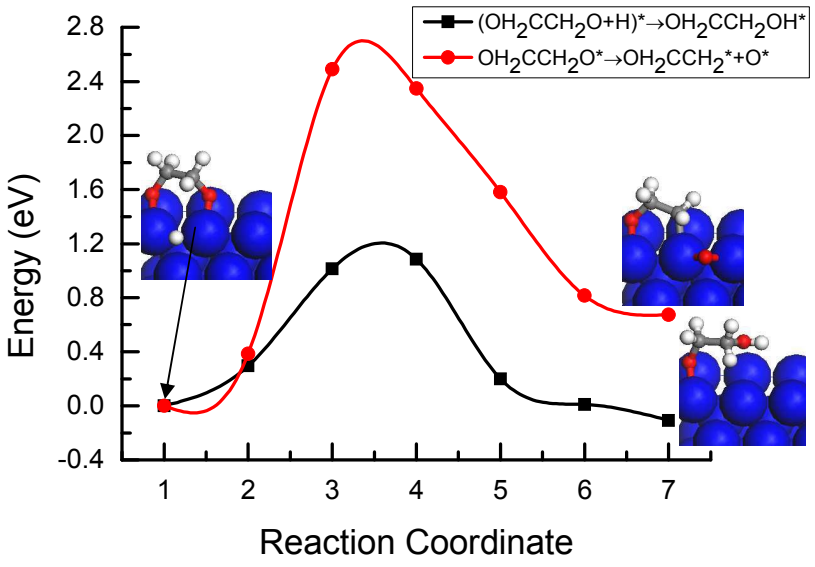


**Fig. 9** Minimum energy paths of further reduction of $OH_2CCH_2O$* intermediate into $OH_2CCH_2OH$* by hydrogenation and $OH_2CCH_2$* on Cu(100) by cleavage of C-O bond, respectively.

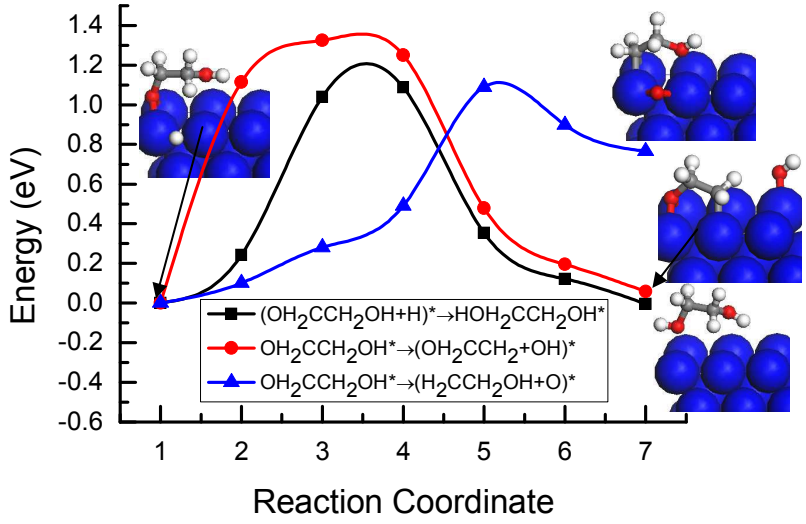


**Fig. 10** Minimum energy paths of further reduction of $OH_2CCH_2OH$* intermediate into $HOH_2CCH_2OH$* by hydrogenation and $OH_2CCH_2$* by dehydroxylation and $H_2CCH_2OH$* by deoxygenation on Cu(100), respectively.

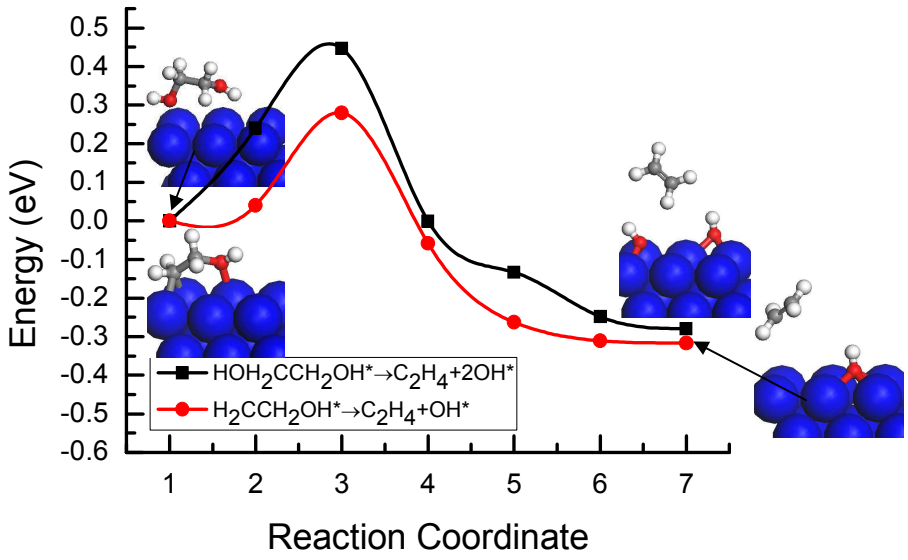


**Fig. 11** Minimum energy paths of further reduction of $HOH_2CCH_2OH^*$ and $H_2CCH_2OH^*$ intermediates into $C_2H_4$ by dehydroxylation on Cu(100), respectively.

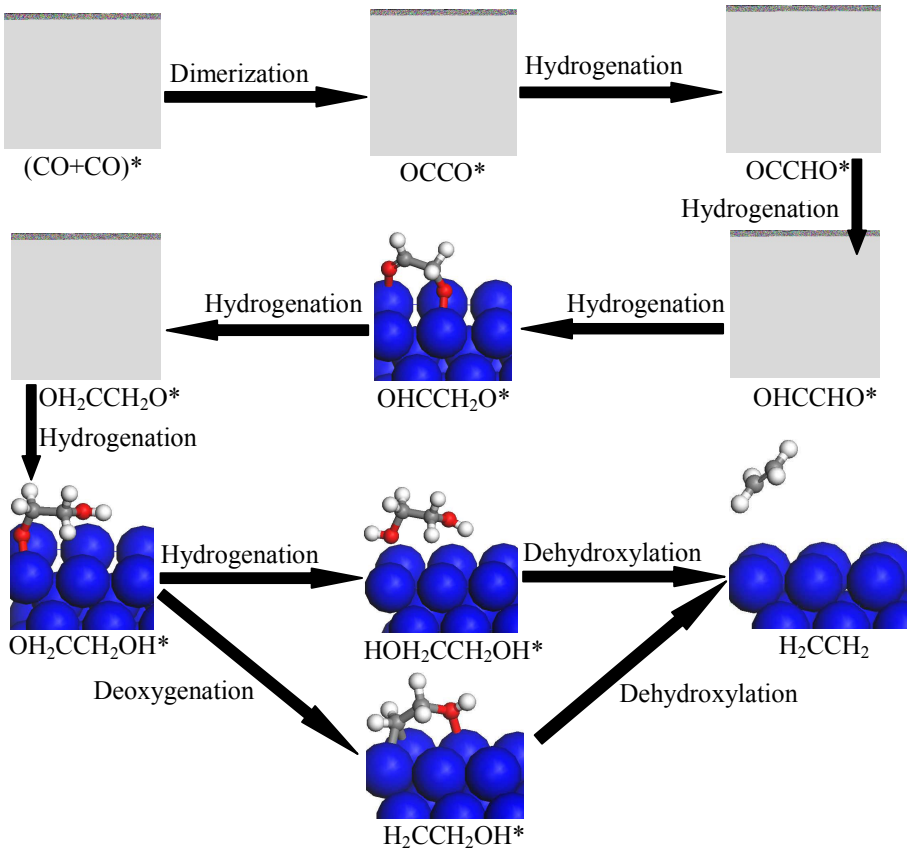


**Fig. 12** Proposed reduction pathways into production $C_2H_4$ in reduction mechanism of CO dimer on Cu(100).